Ionization dynamics via ion-collection field of Rydberg atoms approaching metal surfaces

N. N. Nedeljković*
Faculty of Physics, University of Belgrade, P.O. Box 368, Belgrade, Serbia

D. K. Božanić
Vinča Institute of Nuclear Sciences, P.O. Box 522, Belgrade, Serbia

(Received 27 November 2009; published 22 March 2010)

The ionization dynamics of slow hydrogenlike Rydberg atoms (principal quantum number $n \gg 1$) approaching solid surfaces is considered via an ion-collection electric field, using an appropriate etalon equation method. The complex energy eigenvalue problem is solved in the critical region $R \approx R_c \approx R_c^I$ of the ion-surface distances R in which the ionization process is mainly localized and the parabolic symmetry is preserved. The relatively simple analytical forms for the parabolic rates enable us to elucidate the main features of the self-consistent ionization dynamics of the projectiles with the time-dependent charges. The ionization distances R_c^I are calculated and an agreement of the averaged probability (for the atomic beam) with the corresponding experimental results is discussed for the relevant parameters of the ion-surface system. The formulas are suggested for the simulation of the experimental signal and for deducing the R_c^I values from this signal.

DOI: 10.1103/PhysRevA.81.032902 PACS number(s): 34.35.+a, 34.50.Fa

I. INTRODUCTION

Recently, an interesting problem concerning direct observation of ionization distances R_c^I of Rydberg atoms approaching solid surfaces has attracted considerable attention. This relatively old problem was revisited in the experiments with xenon Rydberg atoms [1–7] and hydrogen molecules [8] approaching a solid surface (with hyperthermal velocities $v \ll 1$ a.u.) in the presence of a weak external electric field F. The experiments [1–7] produced a normalized number of the ionized atoms as a function of the applied electric field F (ion signal). The distances R_c^I were deduced from the values of the minimal electric field $F_{\min}$, which was sufficient to send back the ionized projectile from the beam into detector, by using a simple classical relation between the R_c^I and the $F_{\min}$ values [1]. On the other hand, the ion signal was simulated by employing the model ionization rates in the expression for the averaged ionization probability $\mathcal{P}$ for the atomic beam [3]. We find that the more accurate interpretation of the experimental results (the R_c^I values and the signal shape) can be obtained if the quantum model of ionization is treated simultaneously with the classical law of motion of the projectiles.

The first theoretical study devoted to the ionization dynamics in the presence of an external electric field has been performed within the framework of the complex scaling method (CSM) [9,10]. More recently, time-dependent wave-packet propagation (WPP) studies have been proposed for the same physical problem [11,12]. Along with the CSM and the WPP method, ionization dynamics has been considered as a decay process, using an appropriate etalon equation method (EEM) [13]. According to the decay model, the ionization occurs mainly via electron tunneling localized in the critical region $R \approx R_c \gg 1$ a.u., where the critical distance R_c is the ion-surface distance at which the electron transitions become classically allowed (i.e., when energy term touches the potential barrier top). Using the EEM, the analytical solutions of complex energy eigenvalue problem were obtained for all relevant ion-surface parameters. The ionization distances R_c^I were defined as ion-surface distances at which the ionization probability per unit time (total rate) is maximal. It was demonstrated that the ionization distances belong to the critical region ($R_c^I \approx R_c$).

In the considered case of ionization, the advantage of the EEM is in the fact that the solutions of the eigenvalue problem can be expressed via the solutions of the appropriate etalon equation, which has the same confluent turning points as the original one. Thus, instead of using the expansion over the basis wave functions, characteristic for CSM and WPP method, the eigenfunctions of the EEM can be directly exposed in the parabolic coordinates and classified by a set of parabolic quantum numbers $\mu = (n_1, n_2, m)$. Moreover, the corresponding complex energy spectrum can be obtained directly, without explicit calculation of the eigenfunctions.

In the present article we apply the EEM [13] to study some specific features of the ionization dynamics of the atomic beam important for further understanding of the experimental findings. We consider the decay of an atomic projectile (a representative member of the corresponding quantum subensemble of particles with a given initial velocity) impinging the conducting solid surface in the presence of the ion-collection electric field F. Within the framework of the decay model the active electron is in a decaying state Ψ_μ, while the projectile with the time-dependent charge $q(t)$ moves toward the surface at R-dependent perpendicular velocity $v_\perp(R) = -dR/dt$. Using the EEM, the parabolic ionization rates $\Gamma_\mu(R) = -2\,\mathrm{Im}E_\mu(R)$ and the corresponding energy terms $\mathrm{Re}E_\mu(R)$ are obtained by means of complex eigenenergies $E_\mu(R)$. We restrict our analysis to the high-eccentric surface-oriented Rydberg states (principal quantum number $n = n_1 + n_2 + |m| + 1 \gg 1$), characterized by lower values of the parabolic quantum number n_1 and $m = 0$.

The problem of calculating the ionization probability $P_\mu(R)$ from the rates $\Gamma_\mu(R)$ is resolved in a kind of self-consistent procedure. This problem is nontrivial; namely, in the proposed decay model, the probability $P_\mu(R)$ depends on the projectile

*hekata@ff.bg.ac.rs

motion via perpendicular velocity $v_\perp(R)$ and, simultaneously, the motion of the projectile depends on the ionization probability through the charge $q(t) = Z P_\mu(R)$, where Z is the initial core charge (in atomic units). The ensemble of particles (atomic beam) is treated as a statistical mixture of subensembles with a statistical function $f(v_{\perp 0})$. By taking into account the fact that the field F collects only the projectiles of the beam with $v_{\perp 0} < v_c(\mu, F)$, we define the averaged ionization probability $\mathcal{P}_\mu(F)$; the quantity $v_c(\mu, F)$ is the characteristic function for the proposed ionization dynamics. By using the appropriate expression $\mathcal{P} = \mathcal{P}_\mu(F)$, we are in a position to satisfactorily reproduce the experimental signals without any fitting parameters.

From the ionization probabilities $P_\mu(R)$ we obtain the total rates $\tilde{\Gamma}_\mu = dP_\mu(R)/dt$ of the same narrow width as those of the CSM [9,14] and the WPP method [11,12] (about 50 a.u.), in contrast to the model rates (with widths of about 250 a.u.) used for the simulation of experimental signal in Ref. [3]. By means of the total rates, we get the improved ionization distances R_c^I in comparison to the values calculated in Ref. [13]. We point out that in our previous EEM [13], the perpendicular projectile velocity was taken as constant and the localization of the ionization process has been investigated in a direct, but somewhat approximative manner. Comparing the EEM ionization distances with those that can be deduced from the experiments [1,3], we find that the more accurate values can be obtained if the measured mean fields $\bar{F}$ (with the mean initial perpendicular velocity $\bar{v}$ from the atomic beam) are used instead of the minimal fields $F_{\min}$ combined with the "minimal" value $v_{\perp 0} = 0.7 \times 10^{-5}$ a.u. [1].

This article is organized as follows. In Sec. II we formulate the problem within the framework of the decay model and the EEM, exposing the basic equations for description of the ionization dynamics. In Sec. III we present the self-consistent expression for the ionization probability for the projectile with the time-dependent charge, by including the core motion. In Sec. IV we expose explicit results of the proposed ionization dynamics. The EEM results obtained in the constant perpendicular velocity approximation ($v_\perp = v_{\perp 0}$) are compared with the theoretical predictions of the CSM [9,14] and the WPP method [11,12]. The more general EEM results valid for $v_\perp = v_\perp(R)$ are used for the calculation of the ionization distances and averaged probabilities (signal), which are compared with the experimental findings [1,3]. Some concluding remarks are given in Sec. V.

Atomic units ($e^2 = \hbar = m_e = 1$) will be used throughout the article unless indicated otherwise.

II. FORMULATION OF THE PROBLEM

A. Decay model of ionization dynamics of atomic beam

We consider the ionization of a beam of slow hydrogenlike Rydberg atoms (pointlike core charge $Z = 1$, mass M) impinging a solid surface in a presence of a weak external electric field F (directed from the solid to the vacuum, along the z axis). The ionization dynamics will be analyzed within the framework of an appropriate decay model in which the quantum behavior of the electron transitions and the classical motion of the projectiles are considered simultaneously.

The subensemble of particles with a given initial velocity (with perpendicular component $v_{\perp 0}$) is represented by a single projectile with an active electron in the parabolic Rydberg state state Ψ_μ, where $\mu = (n_1, n_2, m)$ is the set of parabolic quantum numbers and $n = n_1 + n_2 + |m| + 1$. The electronic state Ψ_μ decays during the ionization with the probability $P_\mu(R; v_{\perp 0}, F)$, where R is the instant ion-surface distance. Due to the quantum decay, the "electron cloud" around the projectile core reduces so that the charge q of the initially neutral representative member of the considered subensemble is changing continuously in time; that is, $q = q(t) = q_\mu(R; v_{\perp 0}, F)$. At the time t we have

$$q(t) = Z P_\mu(R). \tag{1}$$

The charge $q(t)$ moves in a presence of solid surface and external field F with the perpendicular velocity $v_\perp = v_\perp(R)$, satisfying the initial condition $v_\perp = v_{\perp 0}$. The presence of different initial velocities of the atomic particles within the beam is considered as a statistical mixture of subensembles, via the statistical function (initial perpendicular velocity distribution) $f(v_{\perp 0})$.

In Fig. 1 we present schematically the described decay model of beam ionization and the corresponding experimental situation [1–7]. The representative projectiles of the subensembles with initial perpendicular velocities $v_{\perp 0} < v_c(\mu, F)$, after the ionization mainly localized at ionization distances $R_c^I(\mu, v_{\perp 0}, F)$, will be collected by the external electric field F and detected experimentally. The corresponding trajectories are characterized by the minimal ion-surface distance $R_{\min}$. The other particles from the atomic beam, after the ionization, enter the near-surface region, where they are neutralized via

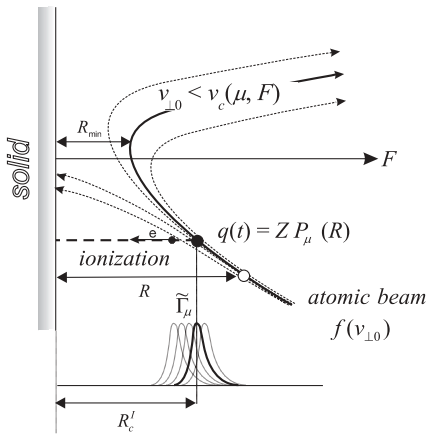

FIG. 1. Decay model of ionization dynamics of the beam of atomic particles, with initial perpendicular velocity distribution $f(v_{\perp 0})$, in the presence of a solid surface and an external electric field F. Each trajectory corresponds to the representative member of the subensemble of Rydberg atoms/ions with a given initial perpendicular velocity $v_{\perp 0}$. The corresponding electronic state Ψ_μ decays during the ionization with the probability $P_\mu(R; v_{\perp 0}, F)$ and the total rate $\tilde{\Gamma}_\mu(R; v_{\perp 0}, F) = dP_\mu/dt$. Only the projectiles with $v_{\perp 0} < v_c(\mu, F)$, after the ionization [mainly localized at ionization distance $R_c^I(\mu, v_{\perp 0}, F)$], will be collected by the external electric field F and detected experimentally.

Auger-type processes. Thus, the representative projectiles with the initial perpendicular velocity $v_{\perp 0}$, can be collected only by the electric fields $F > F_c(\mu, v_{\perp 0})$.

The probabilistic description of the behavior of the representative projectile means that the normalized number of the particles from the beam (with a given initial perpendicular velocity $v_{\perp 0}$), ionized in the interval $[\mathcal{R}, \mathcal{R} + d\mathcal{R}]$, is given by $-dP_\mu(\mathcal{R})$. The charge of the particular particle changes in time in a discrete manner from $q = 0$ to $q = 1$; that is, $q_R(t) = Z\Theta(\mathcal{R} - R)$, where the Θ function $\Theta(x)$ is defined by $\Theta(x) = 0$ for $x < 0$ and $\Theta(x) = 1$ for $x \geqslant 0$. The time-dependent charge $q = q(t)$ given by Eq. (1) represents the subensemble average over different ionic trajectories; namely,

$$\langle q_R(t)\rangle = -\int_0^\infty Z\Theta(\mathcal{R} - R)dP_\mu(\mathcal{R}) = -Z\int_R^\infty dP_\mu(\mathcal{R}) = ZP_\mu(R) = q(t). \quad (2)$$

In Fig. 1, each trajectory is the representative for the manifold of trajectories for the particles ionized at different ion-surface distances. The corresponding beam broadening is taken into account in the proposed decay model as an average effect (see discussion in Sec. IV D).

B. Decay model of the electronic state: Etalon equation method

The quantum model of electron transitions during the ionization is adapted to the critical region $R \approx R_c \gg 1$ a.u. of ion-surface distances R. The critical distance R_c is defined as the distance from the surface at which the electron tunneling is in the very vicinity of the potential barrier top, created between the core and the polarized surface. The ionization distance R_c^I, at which the ionization (per unit time) is the most probable, belongs to the critical region; that is, $R_c^I \approx R_c$. We formulate the problem within the framework of the decay model, using our recently developed EEM [13] to solve the complex energy eigenvalue problem. The choice of potentials relevant to the EEM is extensively discussed in Sec. II A of the Ref. [13]. See also the discussion in Ref. [15].

According to the model, the decaying Rydberg state Ψ_μ of the active electron is considered as an eigenfunction of the Hamiltonian $\hat{H}(R)$,

$$\hat{H}(R)\Psi_\mu(R) = E_\mu(R)\Psi_\mu(R), \quad (3)$$

corresponding to the complex eigenenergy [13]

$$E_\mu(R) = \mathrm{Re}E_\mu(R) - \frac{i}{2}\Gamma_\mu(R), \quad (4)$$

where Γ_μ is the ionization rate. By μ in Eq. (3) we denote the set of approximately good parabolic quantum numbers; that is, we assume that the parabolic symmetry is preserved at intermediate stages of the ionization. That is the case for the experimentally investigated high eccentric Rydberg states, for which the electron transitions are mainly localized in a narrow cylindrical region around the ion-surface axis, so that the corresponding eigenvalue problem (3) can be solved by separating the variables in the parabolic coordinates $\xi = r_A + z_A$, $\eta = r_A - z_A$, and $\varphi = \arctan(y/x)$, where r_A and z_A are the electronic coordinates respective to the atomic core [13]. We shall consider only the decay of the surface-oriented states (lower values of parabolic quantum number n_1), with $m = 0$, which makes our further theoretical analysis more simple, since the "nonadiabatic" transitions are unimportant in that case.

The specific feature of the proposed EEM is that the energies $\mathrm{Re}E_\mu(R)$ and the ionization rates $\Gamma_\mu(R)$ can be obtained without explicit calculation of the wave function $\Psi_\mu(R)$. Details of solving the complex energy eigenvalue problem [Eq. (3)] in the critical region $R \approx R_c$ are given in Ref. [13]. For the ion-surface distances $R \gg R_c$, and for sufficiently small fields, the ionization rates are very small and unimportant for the calculation of the ionization probabilities. The behavior of the energy terms in this region is more interesting, because this behavior could be used in the analysis of the validity of the proposed ionization model. In this far asymptotic region the energy terms can be expressed in the following explicit form [13]:

$$E_{0,\mu} \approx -\frac{Z^2}{2n^2} + \frac{3}{2Z}Fn(n_1 - n_2) + \frac{2Z-1}{4R} - \frac{3}{8}\frac{(Z-1)}{ZR^2}n(n_1 - n_2) + FR. \quad (5)$$

C. Ionization probability $P_\mu(R)$

The full quantum description of the ionization process requires a multichannel model, which includes both the resonant ionization and the neutralization processes, as well as the Auger and radiative processes. Also, the electronic state can be considered as an eigenfunction Ψ_μ of the complex energy eigenvalue problem only if the "adiabatic" conditions are satisfied for all relevant ion-surface distances R. We find that the one-channel ionization model described by the decaying state Ψ_μ is sufficiently accurate for the particular case analyzed in the present article.

First of all, for $R \in [R_{\min}, \infty]$, the Auger-type processes are negligible, because these two-electron processes are localized at smaller ion-surface distances. The radiative processes can be neglected as less probable in comparison to the nonradiative ones. Also, taking into account that the energy terms $\mathcal{E}_\mu = \min(\mathrm{Re}E_\mu, E_{0,\mu})$ of the considered Rydberg states are positioned above the Fermi level of the solid at all relevant ion-surface distances R, we conclude that the resonant neutralization of the previously ionized projectiles by the electron back capture from the solid is also impossible. The criterium of validity of the "adiabatic" approximation within the decay model is somewhat ambiguous, because the states Ψ_μ correspond to the complex eigenenergies E_μ. We assume that the approximation is sufficiently accurate outside of the energy terms crossing region. By analyzing the behavior of the energy terms $\mathcal{E}_\mu$, we concluded that the "adiabatic" approximation is satisfied for $R \in [R_c^I(\mu), \infty]$.

Therefore, the ionization probability $P_\mu(R)$, that is, the probability that the incident atom (the representative member of the subensemble of particles from the atomic beam with a given initial velocity) is ionized at ion-surface distance R, can be obtained using the one-channel rate equation approach and the supposition of classical law of ionic motion. The probability for an incidence atom to survive the passage to a distance R from surface is given by the quantity $1 - P_\mu(R)$. As

a solution of the rate equation, for the ionization probability $P_\mu(R)$ of the occupied electronic state $\mu = (n_1, n_2, m)$ we obtain the relation

$$P_\mu(R) = 1 - \exp\left[-\int_R^\infty \frac{\Gamma_\mu(R)}{v_\perp(R)} dR\right], \tag{6}$$

valid for $R > R_{\min}(\mu, v_{\perp 0}, F)$, where $R_{\min}$ is the minimal ion-surface distance for a given μ, $v_{\perp 0}$, and F (see Fig. 1). The intermediate stages of ionization are characterized by the total ionization rates

$$\tilde{\Gamma}_\mu(R) = \frac{dP_\mu}{dt} = -v_\perp(R)\frac{dP_\mu(R)}{dR}. \tag{7}$$

The positions of the maxima of the total ionization rates can be considered as ionization distances $R_c^I(\mu, v_{\perp 0}, F)$; that is, $(d\tilde{\Gamma}_\mu/dR)_{R_c^I} = 0$.

III. SELF-CONSISTENT EEM EXPRESSION FOR THE IONIZATION PROBABILITY

A. EEM ionization probability $P_\mu(R)$ with inclusion of core motion

The probability $P_\mu(R)$, defined by Eq. (6), depends on the ionic motion via perpendicular velocity $v_\perp(R)$. At the same time, the motion of the atomic projectile (representative member of the considered subensemble) depends on the ionization probability via the charge $q = q(t) = ZP_\mu(R)$. Therefore, a kind of self-consistent procedure is necessary for solving the problem.

The charge q moves toward the surface in the external electric field F. For the physical conditions considered in the present article, the dynamical response of the conducting solid surface reduces to the classical image forces. Thus, the charge q experiences the classical image acceleration and at the same time the opposite effect of the external electric field. According to Eq. (1) the velocity $v_\perp(R)$ depends on $P_\mu(R)$, and vice versa, the $P_\mu(R)$ depends on $v_\perp(R)$ according to Eq. (6).

We resolve the problem by including the R-dependent expression for the perpendicular velocity into the expression for the ionization probability iteratively. That is, in the ith iterative step ($i = 0, 1, 2, \ldots$) we assume that

$$P_\mu^{(i)}(R) = 1 - \exp\left[-\int_R^\infty \frac{\Gamma_\mu(R)}{v_\perp^{(i)}(R)} dR\right], \tag{8}$$

where, for $i = 1, 2, \ldots$,

$$v_\perp^{(i)2}(R) = v_{\perp 0}^2 - \frac{2FZ}{M}\int_R^\infty P_\mu^{(i-1)}(R)dR + \frac{Z^2}{2M}\int_R^\infty \frac{P_\mu^{(i-1)2}(R)}{R^2}dR, \tag{9}$$

and, for $i = 0$, $v_\perp^{(0)} = v_{\perp 0}$ is the initial perpendicular velocity. We point out that the accurate treatment of the projectile motion is essential for the analysis of the ion signal (Sec. IV D).

Two important facts concerning the motion of the representative projectile follow from the proposed iterative procedure. First, for a given $v_{\perp 0}$ and $F > F_c$, from the relation $v_\perp(R_{\min}) = 0$, we obtain the minimal ion-surface distance $R_{\min}$; in the iterative step for which the iterative procedure is practically finished ($i = i_f$), we get

$$1 = \frac{2FZ}{Mv_{\perp 0}^2}\int_{R_{\min}}^\infty P_\mu^{(i_f-1)}(R)dR - \frac{Z^2}{2Mv_{\perp 0}^2}\int_{R_{\min}}^\infty \frac{P_\mu^{(i_f-1)2}(R)}{R^2}dR. \tag{10}$$

Second, the critical electric field $F_c(\mu, v_{\perp 0})$, that is, the minimal field necessary for collecting the projectiles with a given initial perpendicular velocity $v_{\perp 0}$, can be obtained from Eq. (10) as a minimal F for which this equation has a real and positive solution for $R_{\min}$. The fact that for all $v_{\perp 0}$ the critical field $F_c(\mu, v_{\perp 0})$ exists means that for all F there exists a maximal value $v_c(\mu, F)$ of the $v_{\perp 0}$ for which the projectiles can be collected by the field F (see Fig. 1).

The iterative procedure gives the final expressions for the ionization probabilities and the corresponding total rates. From these values one can derive the accurate expressions for the ionization distances R_c^I. These values enable us to formulate the steplike approximation for the ionization probability.

B. Steplike probability $P_\mu^{\text{step}}(R)$

Within the framework of a steplike approximation for the subensemble of particles with a given initial velocity, one can assume that $\Gamma_\mu = 0$ for $R > R_c^I$ and $\Gamma_\mu = \infty$ for $R < R_c^I$. In this approximation, prior to ionization, the ionic core of the representative projectile is completely screened by the active electron; that is, $q(t) = 0$, so that $v_\perp(R) \approx v_{\perp 0}$ for $R > R_c^I$. At $R = R_c^I$ the atomic projectile is completely and instantaneously ionized, so that $q(t) = Z = 1$ for $R < R_c^I$. Note that $R_c^I = R_c^I(\mu, v_{\perp 0}, F)$.

In the considered steplike approximation we have

$$P_\mu^{\text{step}}(R) = \Theta\left(R_c^I - R\right). \tag{11}$$

Now, for $i = i_f$ and $P_\mu^{(i_f-1)} = P_\mu^{\text{step}}$, the law of motion of the ionic projectile, given by Eq. (9), can be expressed explicitly. For $R < R_c^I$ we have

$$v_\perp^2(R) \approx \frac{2}{M}\left(a + \frac{Z^2}{4R} + ZFR\right), \tag{12}$$

where $a = T_{\perp 0} - Z^2/4R_c^I - ZFR_c^I < 0$, $Z = 1$, and $T_{\perp 0} = Mv_{\perp 0}^2/2$ is the initial "perpendicular" projectile kinetic energy. Using the condition $v_\perp(R_{\min}) = 0$, the distances $R_{\min}$ of the projectile's closest approach to the surface can be obtained from Eq. (12) [or Eq. (10) in the steplike approximation]. We get

$$R_{\min} = -\frac{a}{2ZF} + \frac{1}{2ZF}\sqrt{a^2 - Z^3F}. \tag{13}$$

The critical field F_c, that is, the minimal electric field for which $R_{\min}$ exists ($a^2 - Z^3F \geqslant 0$), is given by $F_c \approx (\sqrt{Z}/2R_c^I + \sqrt{T_{\perp 0}/ZR_c^I})^2$ [9]. We note that the approximative character of the former expression is in the assumption that R_c^I is independent of F. For $F = F_c$, we have that $a^2 - Z^3F = 0$, so that the corresponding minimal ion-surface distance is given by the following simple relation: $R_{\min} = \sqrt{Z/4F_c}$.

In the steplike approximation, the electric field F_c is directly related with the ionization distance R_c^I and $v_{\perp 0}$. Thus,

if the field F_c could be measured, one can calculate the ionization distances R_c^I from the following simple classical relation [1–7]:

$$R_c^I = \frac{T_{\perp 0}}{4F_c}\left(1+\sqrt{1+\frac{2\sqrt{F_c}}{T_{\perp 0}}}\right)^2. \tag{14}$$

Expressing the $v_{\perp 0}$ via F_c, from Eq. (14) we obtain the explicit expression for the velocity v_c via F:

$$v_c = \sqrt{\frac{2ZR_c^I F}{M}} - \sqrt{\frac{Z^2}{2MR_c^I}}. \tag{15}$$

Equation (15) is obtained under the assumption that the R_c^I value used in the steplike model is almost independent on $v_{\perp 0}$. Note that in the analyzed experiments [1–7] the measured values of minimal fields $F_{\min}$ would correspond to the F_c only for a monoenergetic atomic beam.

The steplike approximation can also be formulated for the particular member of the particle subensemble, which is ionized at arbitrary distance $\mathcal{R}$ from the surface: In that case we have $P_\mu^{\text{step}}(R) = \Theta(\mathcal{R} - R)$. The trajectory of the considered particle is also characterized by the minimal ion-surface distance $R_{\min,R}$, which is now given by Eq. (13), in which we replace R_c^I with $\mathcal{R}$. The quantity $R_{\min,R}$ exists for $v_{\perp 0} < v_{c,R}(\mathcal{R}, F)$, where the quantity $v_{c,R}(\mathcal{R}, F)$ is given by Eq. (15) for $R_c^I \to \mathcal{R}$. It means that the considered particular member of the subensemble will be collected by the field F, if it is ionized at distance $\mathcal{R} > R_{c,R}(v_{\perp 0}, F)$, where $R_{c,R}(v_{\perp 0}, F)$ is given by Eq. (14) for $F_c \to F$.

IV. RESULTS

A. Intermediate stages of ionization in the constant-velocity approximation

As a first step toward a direct comparison with experimental signals, we consider the ionization rates $\Gamma_\mu(R)$ and energies $\mathrm{Re}E_\mu(R)$, as well as the ionization probabilities $P_\mu(R)$ and total rates $\tilde{\Gamma}_\mu(R)$, at intermediate stages of the process (for $R \approx R_c$). In order to compare our predictions with other available theoretical models (CSM and WPP), in some cases the principal quantum numbers n and the values of the external electric fields F will be out of the range relevant for experiments. In exposing the EEM vs CSM and the WPP method results, the ionization probabilities and the total rates are calculated in the zero approximation ($i = 0$), assuming that $v_\perp \approx v_{\perp 0}$.

In Fig. 2 we present the EEM ionization rates $\Gamma_\mu(R)$ and energy terms $\mathrm{Re}E_\mu(R)$ for $n = 13$, 15, 17, and 20, for $n_1 = m = 0$, and for two values of the external electric field: $F = 0$ and $F = 10^{-6}$ a.u. The values of the rates and energies at the ion-surface distances R_c are indicated by circles. From Fig. 2(a) we recognize that the ionization rates corresponding to different values of the principal quantum number n are localized at different ion-surface distances R; obviously, the curves corresponding to higher n are positioned at larger R. The energy terms presented in Fig. 2(b) show the decreasing behavior with decreasing R, for $R \approx R_c$. At larger R the energy terms are given by the asymptotic expression $E_{0,\mu}$, given by Eq. (5). These terms (not shown) monotonically increase with

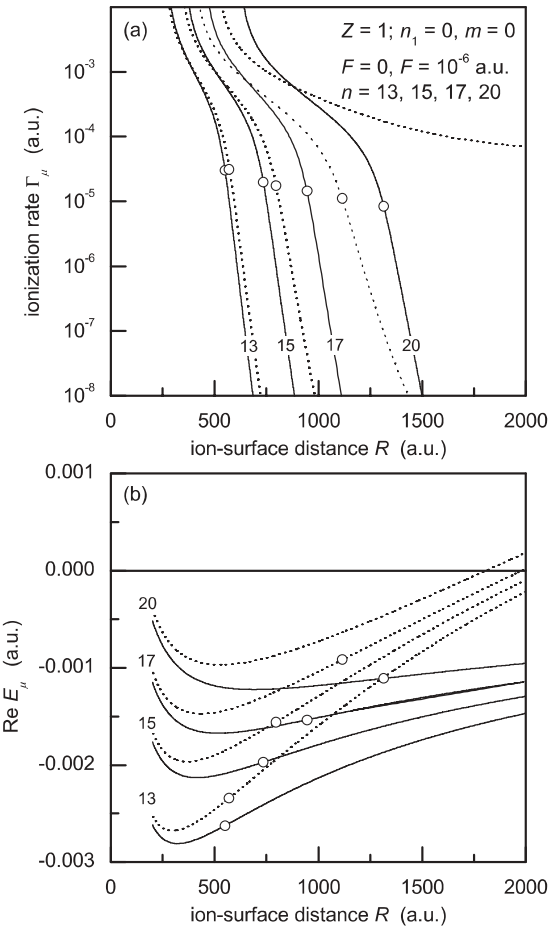

FIG. 2. (a) Ionization rates $\Gamma_\mu(R)$ and (b) energy terms $\mathrm{Re}E_\mu(R)$ for $n = 13$, 15, 17, and 20, for $n_1 = 0$ and $m = 0$, in the external electric fields $F = 0$ and $F = 10^{-6}$ a.u. (solid and dotted curves, respectively). Circles indicate the positions of critical distances R_c.

decreasing R (see Figs. 3(c), 4(c), 5(c), and 6(c) in Ref. [13]). The energy levels presented in Fig. 2(b) (and also the levels $E_{0,\mu}$) are positioned far above the Fermi level of the conducting surfaces (the typical value of the solid work function is $\phi = 5$ eV; i.e., $\phi = 0.184$ a.u.).

The presence of an electric field shifts the rates toward the larger ion-surface distances R [compare the dotted and the solid curves in Fig. 2(a)], while the energy terms shift upward with the increase of F [compare the dotted and the solid curves in Fig. 2(b)]. The obtained rates and energy terms, for the two considered electric fields, can be compared with the corresponding CSM quantities. In our previous article [13] it was demonstrated that the EEM rates and energy terms follow the results of the available CSM ($n = 10$ and $F \neq 0$ [9,10], $n = 10$ and $F = 0$ [16], and $n = 15$ and $F = 0$ [14]).

The ionization probabilities $P_\mu(R)$ and the total rates $\tilde{\Gamma}_\mu(R)$, scaled by $v_{\perp 0}$, for two different values of the external electric field ($F = 0$ and $F = 10^{-6}$ a.u.) are given in Fig. 3. For the initial perpendicular velocity the value $v_\perp = v_{\perp 0} = 10^{-5}$ a.u. was taken. In Fig. 3(b) we also present the CSM total rate calculated from the available data for the ionization rate for $n = 15$ and $F = 0$ [14]. With increasing n both the probabilities and total rates are shifted toward the larger

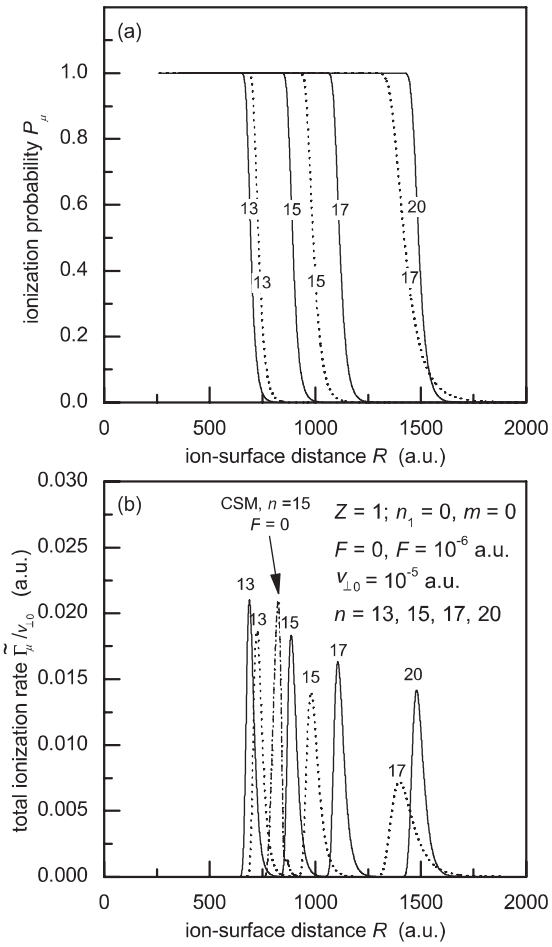

FIG. 3. (a) Ionization probabilities $P_\mu(R)$ and (b) total rates $\tilde{\Gamma}_\mu(R)/v_{\perp 0}$ for $n = 13$, 15, 17, and 20, for $n_1 = 0$ and $m = 0$, in the external electric fields $F = 0$ and $F = 10^{-6}$ a.u. (solid and dotted curves, respectively). The perpendicular ionic velocity is $v_\perp = v_{\perp 0} = 10^{-5}$ a.u. The dot-dashed curve in (b) is the total rate for $n = 15$ and $F = 0$, calculated from the CSM rate [14].

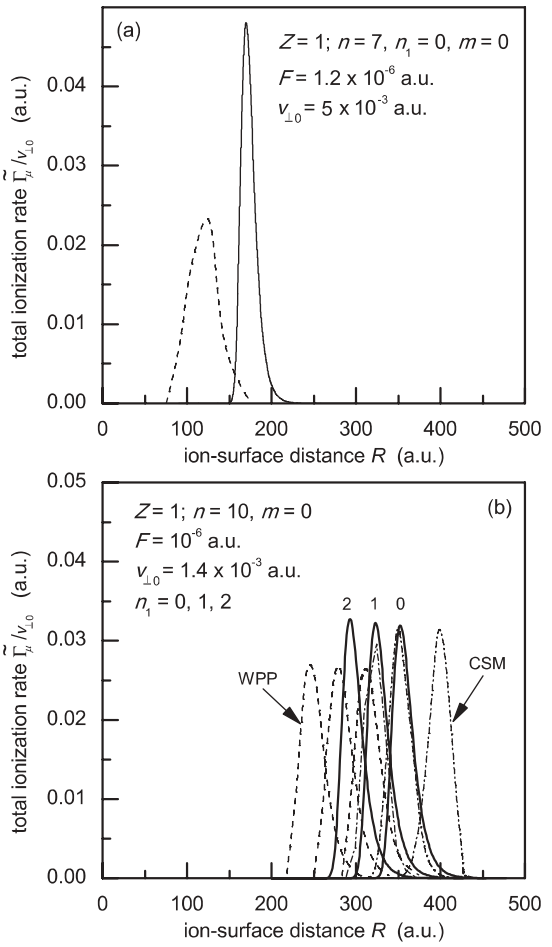

FIG. 4. Total ionization rates $\tilde{\Gamma}_\mu(R)/v_{\perp 0}$ (solid curves) for (a) $n = 7, n_1 = 0, m = 0$, $F = 1.2 \times 10^{-6}$ a.u., and $v_{\perp 0} = 5 \times 10^{-3}$ a.u., and (b) $n = 10$, $n_1 = 0$, 1, and 2, $m = 0$, $F = 10^{-6}$ a.u., and $v_{\perp 0} = 1.4 \times 10^{-3}$ a.u. Dashed curves are the WPP method results for (a) the Xe($n = 7$) ions [11] and (b) the H($n = 10$) ions [12]; dot-dashed curves in (b) are the total rates calculated from the CSM rates [9].

ion-surface distances R; this effect is well known and recognized within all the theoretical approaches and models. The inclusion of the external electric field shifts the probabilities and total rates toward the larger ion-surface distances R (compare the dotted and the solid curves in Fig. 3). The positions of maxima of the total rates presented in Fig. 3(b) determine the ionization distances R_c^I in the zero-order ($i = 0$) approximation.

In Figs. 4(a) and 4(b) we present the total ionization rates $\tilde{\Gamma}_\mu(R)/v_{\perp 0}$ (solid curves), for the Rydberg states $\mu = (n = 7,\ n_1 = 0,\ m = 0)$ and $\mu = (n = 10,\ n_1 = 0\text{–}2,\ m = 0)$, respectively, for the external electric fields and initial perpendicular atomic velocities relevant for comparison with the WPP results (dashed curves) [11,12]. Also, in Fig. 4(b) we present the total rates calculated from the available CSM ionization rates results (dot-dashed curves) [9]. We point out that the considered velocities are significantly larger than that used in Fig. 3, and also in Sec. IV D, where we compare the EEM with the available experiments. From the figure we see that in all cases the EEM curves are positioned at larger ion-surface distances in comparison to the WPP predictions and at smaller distances compared to the positions of the CSM rates. However, the EEM, WPP, and CSM rates are all bell shaped and of similar widths (≈50 a.u.). This indicates that all considered theoretical models imply strong localization of the ionization process, with well-defined positions of maxima of total ionization rates.

With the increase of n_1 the total rates shift toward the smaller ion-surface distances R [see Fig. 4(b)]. In some cases this shift is larger than the shift induced by the external electric field F.

B. Simultaneous treatment of the ionization and the projectile motion

In order to perform a direct comparison of our EEM predictions with the experimental findings (ionization distances and ion signals), it is necessary to include the fact that the perpendicular velocity $v_\perp$ of the representative projectile, with charge $q = q(t) = Z P_\mu(R)$, is changing during the ionization.

The results of the iterative procedure for the simultaneous treatment of the ionization probability and the projectile motion, expressed by Eqs. (8) and (9), is illustrated in Figs. 5(a) and 5(b). We present the probabilities $P_\mu^{(i)}$ and the perpendicular velocities $v_\perp^{(i)}$ in the ith iterative step ($i = 0$, 1 and 2) as a function of the ion-surface distances R for the Rydberg state with principal quantum number $n = 17$, and for some characteristic values of the external electric field F [the values of the field are given in Figs. 5(a) and 5(b)]. For the initial perpendicular velocity we take the value $v_{\perp 0} \equiv \bar{v} = 1.4 \times 10^{-5}$ a.u., which represents the mean velocity of the experimental beam [3].

It can be seen that the iterative procedure rapidly converges. The probabilities for $i = 2$ are slightly shifted toward the larger ion-surface distances R in comparison to the zero-order ($i = 0$) curves [see Fig. 5(a)]; thus, $R_c^{I(i)} \gtrsim R_c^{I(0)}$. From Fig. 5(b) we recognize that the minimal ion-surface distances $R_{\min}$ [zero of the function $v_\perp = v_\perp(R)$] exists for the electric fields $F = 4 \times 10^{-7}$ a.u. and $F = 5 \times 10^{-7}$ a.u., whereas the field $F = 3 \times 10^{-7}$ a.u. is insufficient to collect the ions with the considered initial perpendicular velocity (represented by one projectile within the framework of the considered decay model). The critical field for the given Rydberg state and velocity is $F_c = 3.4 \times 10^{-7}$ a.u. Also, comparing Figs. 5(a) and 5(b), an important fact that $P_\mu(R_{\min}) \approx 1$ can be observed.

In Fig. 5(c) we present the minimal ion-surface distances $R_{\min}$ via F for the Rydberg state $\mu = (n = 17,\ n_1 = 0,\ m = 0)$. We consider the closest approach to the surface of the (representative) projectiles for three characteristic initial perpendicular velocities: $v_{\perp 0} = 0.7 \times 10^{-5}$ a.u, $v_{\perp 0} = 1.4 \times 10^{-5}$ a.u., and $v_{\perp 0} = 2.1 \times 10^{-5}$ a.u. The curves are obtained within the framework of iterative procedure ($i = 2$), by solving Eq. (10). We point out that each curve begins at $F = F_c(\mu, v_{\perp 0})$.

In Fig. 6 we expose the relation (for $i = 2$) between the critical velocity v_c and the external electric field F, characteristic for the ionic motion treated simultaneously with the surface ionization (decay of the state μ). We recall that the value $v_c(\mu, F)$, for the given μ and F, represents the maximal value of the initial perpendicular velocity $v_{\perp 0}$, for which the solution of Eq. (10) exists in a real domain. The graph shown in Fig. 6 (for $F = F_c$ and $v_c = v_{\perp 0}$) also gives the critical field $F_c(\mu, v_{\perp 0})$: the minimal field for which $R_{\min}$ exists for the given μ and $v_{\perp 0}$. The relation between the quantities v_c and F, that is, the F_c and the $v_{\perp 0}$, play an essential role in our theoretical explanation of the experimental signal. We note that the critical velocities $v_c(\mu, F)$ are close to those obtained by the steplike model formula for the ensemble [Eq. (15)] if the decay model values for R_c^I are assumed.

C. Ionization distances

The ionization distances R_c^I we obtain by treating the probabilities and the total rates in the i_f order. Due to the screening of the core charge for $R > R_c^I$, the obtained ionization distances are very close to those in the zero order ($i = 0$).

In Fig. 7(a) we present the ionization distances R_c^I, via an external electric field F, for the Rydberg states μ with $n = 13$, 15, 17, and 20, and $n_1 = m = 0$. The quantities R_c^I are obtained from the relation $(d\tilde{\Gamma}_\mu/dR)_{R_c^I} = 0$, within the framework of the EEM in the $i = 2$ iterative step. The results are presented for characteristic values of the initial perpendicular ionic

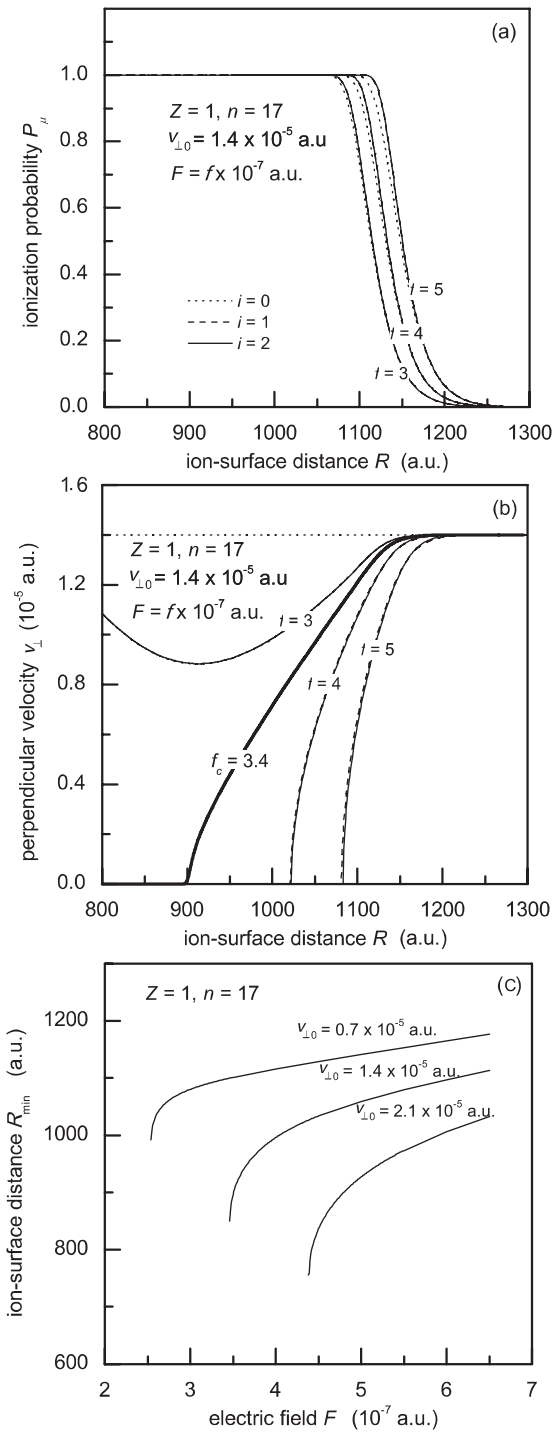

FIG. 5. Decay of the Rydberg state $\mu = (n = 17,\ n_1 = 0,\ m = 0)$. (a) Ionization probabilities $P_\mu^{(i)}(R)$ for $i = 0$, 1, and 2 of the representative atomic projectile ($Z = 1$) impinging the solid surface with the initial perpendicular velocity $v_{\perp 0} = 1.4 \times 10^{-5}$ a.u in the external electric field F. (b) The corresponding velocities $v_\perp^{(i)}(R)$. The curve for the critical field $F = F_c = 3.4 \times 10^{-7}$ a.u. separates the types of projectile motion. Each curve for $F > F_c$ intersects the R axis at $R = R_{\min}$. (c) Minimal ion-surface distances $R_{\min}$ via F for $v_{\perp 0} = 0.7 \times 10^{-5}$ a.u., $v_{\perp 0} = 1.4 \times 10^{-5}$ a.u., and $v_{\perp 0} = 2.1 \times 10^{-5}$ a.u. Each curve begins at $F = F_c(\mu, v_{\perp 0})$.

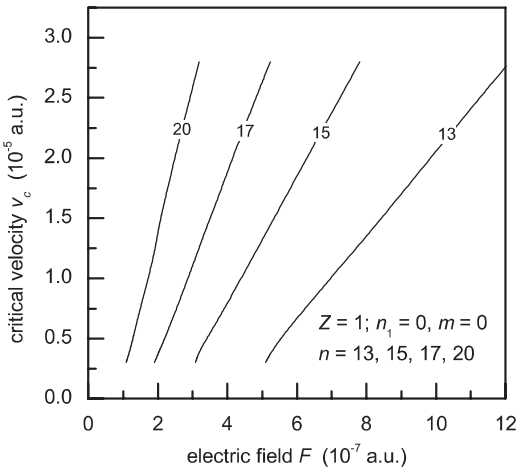

FIG. 6. Critical velocity $v_c(\mu, F)$ via an external electric field F for ionization of the representative atomic projectiles ($Z = 1$) prepared in the state $\mu = (n, n_1 = 0, m = 0)$, where $n = 13$, 15, 17, and 20. For $v_c = v_{\perp 0}$ and $F = F_c$, we get the critical electric field $F_c(\mu, v_{\perp 0})$.

velocities for the experimental beam: $v_{\perp 0} = 0.7 \times 10^{-5}$ a.u, $v_{\perp 0} = 1.4 \times 10^{-5}$ a.u., and $v_{\perp 0} = 2.1 \times 10^{-5}$ a.u. Each curve begins at $F = F_c(\mu, v_{\perp 0})$. We point out that the presented ionization distances are more accurate in comparison to the EEM values calculated in Ref. [13].

The obtained R_c^I values can be compared with the ionization distances deduced from the experimentally available minimal values $F_{\min}$ of the applied electric field F, necessary for collecting the ionized particles of the projectile beam [1–7]. In the cited experiments, the initial atomic states have been prepared by the laser field, which was polarized perpendicular to the surface to selectively populate the $m = 0$ state. Two different initial states have been considered: the Rydberg state with $n_1 \approx 0$ ("Stark state" oriented toward the surface; the most "red state") and in the state with $n_1 \approx n - 1$ (Rydberg state oriented from the surface toward the vacuum; the most "blue state"). As already discussed, the present EEM, without inclusion of the nonadiabatic effects, is suitable for explanation of the first situation, the case $n_1 \approx 0$.

In Fig. 7(b) with solid squares we show the EEM ionization distances corresponding to the experimental values of the minimal external electric field $F_{\min}(\mu)$ for the projectile beam of the atomic particles prepared in the state $\mu = (n, n_1 = 0, m = 0)$; for these states $n_2 = n - 1$. According to Ref. [1], the values $F_{\min}(\mu)$ for $n = 13$, 15, 17, and 20 are $F_{\min}(n = 13) = 5.6 \times 10^{-7}$ a.u., $F_{\min}(n = 15) = 3.0 \times 10^{-7}$ a.u., $F_{\min}(n = 17) = 1.9 \times 10^{-7}$ a.u., and $F_{\min}(n = 20) = 2.0 \times 10^{-7}$ a.u. We consider the ionization distances for the initial perpendicular velocities $v_{\perp 0} = 0.5 \times 10^{-5}$ a.u., $v_{\perp 0} = 0.4 \times 10^{-5}$ a.u., $v_{\perp 0} = 0.3 \times 10^{-5}$ a.u., and $v_{\perp 0} = 0.4 \times 10^{-5}$ a.u. for the Rydberg states with $n = 13$, 15, 17, and 20, respectively. For the chosen values of the quantity $v_{\perp 0}$, the fields $F_{\min}$ represent the critical fields F_c; that is, $v_{\perp 0} = v_c(\mu, F_{\min})$ (see Fig. 6). Note that in Ref. [13], the ionization distances in all cases was for the initial perpendicular velocity $v_{\perp 0} = 10^{-5}$ a.u.

In the steplike approximation the R_c^I values for $F = F_{\min}$ and $v_{\perp 0} = v_c(\mu, F_{\min})$ are expressed by Eq. (14) [1]. These

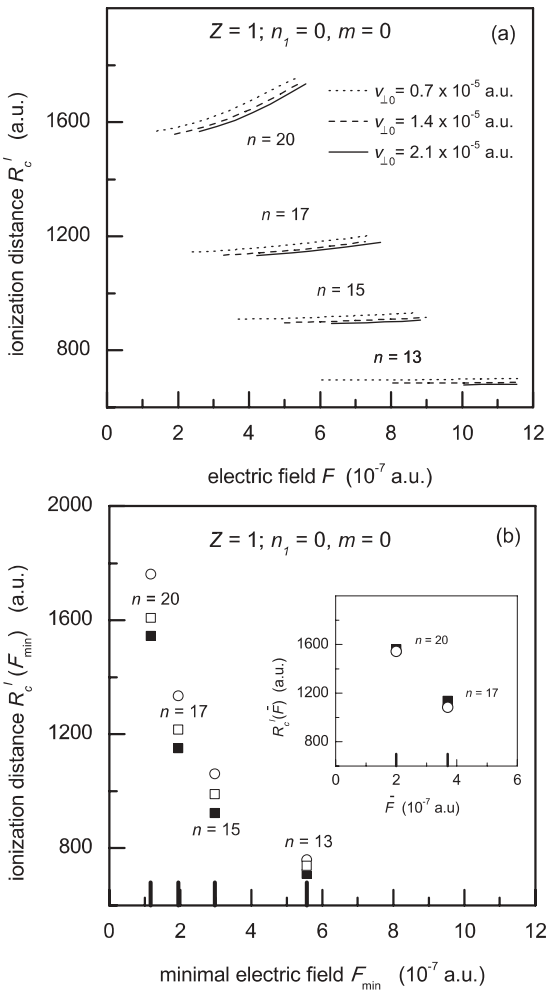

FIG. 7. (a) Ionization distances R_c^I via an external electric field F for the initial perpendicular projectile velocities $v_{\perp 0}$ indicated in the figure. Each curve begins at $F = F_c(\mu, v_{\perp 0})$. (b) Ionization distances R_c^I for the minimal fields $F = F_{\min}$ obtained experimentally and for $v_{\perp 0} = v_c(\mu, F_{\min})$ taken from Fig. 6; the EEM and the steplike model values are represented by the solid and open squares, respectively. Circles represent the "experimental" data [Eq. (14) for $F = F_{\min}$ and $v_{\perp 0} = 0.7 \times 10^{-5}$ a.u.] [1]. (Inset) Solid squares and circles are the ionization distances obtained by the EEM and from Eq. (14), respectively, for the experimental values $F = \bar{F}$ [3] and $v_{\perp 0} = \bar{v} = 1.4 \times 10^{-5}$ a.u.

ionization distances, shown as open squares in Fig. 7(b), are relatively close to those predicted by the EEM (solid squares). We point out that Eq. (14) for the experimental values $F_{\min}$ in the combination with $v_{\perp 0} \approx 0.7 \times 10^{-5}$ a.u. has been used in Ref. [1] for the calculation of the ionization distances. The so-obtained values [circles in Fig. 7(b)] are larger than the EEM values.

The discussion presented in this section leads to the conclusion that the considered experiments [1–7] could be used for deducing the ionization distances from Eq. (14) with the measured minimal fields $F = F_{\min}$, provided that the values $v_{\perp 0} = v_c(\mu, F_{\min})$ are also known. However, these values are not available experimentally, which induces a difficulty in a direct correlation between the experiments (ion signal) and the ionization distances. By measuring the mean

electric field $\bar{F}$ (see Sec. IV D) instead of $F_{\min}$, and calculating the R_c^I for the mean velocities $\bar{v}$ by Eq. (14), the error in deducing the R_c^I values from the experiment can be minimized. The agreement of the so-calculated R_c^I values (circles) and the EEM predictions (solid squares) is demonstrated in the inset in Fig. 7(b), in which we present the cases $n = 17$ and $n = 20$, for which the experimental mean values $\bar{F}$ are available. The experiment [3] gives the values $\bar{F} = 3.7 \times 10^{-7}$ a.u. and $\bar{F} = 2.0 \times 10^{-7}$ a.u. for $n = 17$ and $n = 20$, respectively, while the mean initial perpendicular velocity of the beam is $\bar{v} \approx 1.4 \times 10^{-5}$ a.u.

D. Ion signal

Using the results of Secs. IV A and IV B, we are in a position to analyze the experimental signals; among the available experimental results [1–7], we consider only those that concern the normalized ion signal for the interaction of Rydberg atoms with conducting, absolutely flat surfaces [3]. Also, our analysis of the signal is restricted to the Rydberg atoms prepared in the state $\mu = (n, n_1 = 0, m = 0)$.

We find that the fraction of the incident Rydberg atoms, finally collected by the field F and detected in experiments, that is, the normalized ion signal as a function of the applied field, can be compared with the averaged probability,

$$\mathcal{P}_\mu(F) = \int_{-\infty}^{v_c(\mu,F)} f(v_{\perp 0}) P_\mu(R_{\min}; v_{\perp 0}, F) dv_{\perp 0}. \quad (16)$$

The function $f(v_{\perp 0})$, satisfying the relation $\int_{-\infty}^{\infty} f(v_{\perp 0}) dv_{\perp 0} = 1$, represents the initial distribution of the perpendicular velocity $v_{\perp 0}$. By the upper bound $v_c(\mu, F)$ in the integral in Eq. (16) we take into account the previously discussed fact that (for the given μ and F), only the ions with $v_{\perp 0} < v_c$ are detected. Extension of the range of integration in Eq. (16) to $-\infty$ is for convenience. We note that at minimal ion-surface distances $R_{\min}$ we have $P_\mu(R_{\min}; v_{\perp 0}, F) \approx 1$ in the range of integration in Eq. (16) and for the majority of the considered electric fields (see Fig. 5).

By Eq. (16) we express the normalized number of collected ions obtained within the framework of the decay model, considering the atomic beam as a statistical mixture of subensembles of particles with a given initial velocity. That is, we perform an averaging over the $v_{\perp 0}$ of the normalized number of collected particles from the corresponding subensemble. Each subensemble is represented by a single moving projectile, consisting of the active electron in the Rydberg state Ψ_μ and the ionic core with charge $Z = 1$. Due to quantum decay of the electronic state Ψ_μ, with the probability $P_\mu(R; v_{\perp 0}, F)$ given by Eq. (8), the projectile charge $q(t) = q_\mu(R; v_{\perp 0}, F)$ is changing continuously in time: $q(t) = Z P_\mu(R) = \langle q_R(t) \rangle$ [Eqs. (1) and (2)]. The character of the motion of the representative projectile determines the probability of detection (normalized number of collected ions).

On the other hand, we can consider the behavior of the particular members of the subensemble, characterized by the quantities $R_{cR}(v_{\perp 0}, F)$ and $v_{cR}(\mathcal{R}, F)$ defined in Sec. III B, assuming that the number of particles ionized in the interval $[\mathcal{R}, \mathcal{R} + d\mathcal{R}]$ is given by $-dP_\mu(\mathcal{R})$. In the considered case, the normalized number of collected particles from the subensemble and the ensemble are, respectively, given by $-\int_{R_{cR}}^{\infty} dP_\mu(\mathcal{R}) = P_\mu(R_{cR}; v_{\perp 0}, F)$ and [3–7]

$$\mathcal{P}_\mu(F) = \int_{-\infty}^{\infty} f(v_{\perp 0}) P_\mu(R_{cR}; v_{\perp 0}, F) dv_{\perp 0}. \quad (17)$$

In the steplike approximation for the subensemble, the ionization probability is expressed by Eq. (11), so that $P_\mu(R_{cR}) = \Theta(R_c^I - R_{cR}) = \Theta\mathbf{(}v_c(\mu, F) - v_{\perp 0}\mathbf{)}$, where the critical velocity $v_c(\mu, F) = v_{cR}(R_c^I, F)$ is expressed via the ionization distance R_c^I by Eq. (15). Therefore, taking into account that [for the appropriate $R_c^I(\mu, v_{\perp 0}, F)$ value] the quantity $v_c(\mu, F)$ expressed by Eq. (15) is close to the critical velocity $v_c(\mu, F)$ calculated in our decay model, we see that Eq. (17) turns into Eq. (16).

Note that the averaged probability given by Eq. (17) can be expressed in the form in which the beam broadening is exposed more explicitly: $\mathcal{P}_\mu(F) = \int_0^{\infty} \int_{-\infty}^{v_{cR}(\mathcal{R},F)} f(v_{\perp 0})[-dP_\mu(\mathcal{R})/d\mathcal{R}] dv_{\perp 0} d\mathcal{R}$. By replacing the quantity $v_{cR}(\mathcal{R}, F)$ with the appropriate mean $v_{cR}(R_c^I, F) = v_c(\mu, F)$, and using for the critical velocity $v_c(\mu, F)$, the value obtained within the framework of the decay model, again we get the expression (16). Since $v_{cR}(\mathcal{R}, F) \lessgtr v_c(\mu, F)$ for $\mathcal{R} \lessgtr R_c^I$, and taking into account that the integration over $\mathcal{R}$ is localized in a narrow interval around the $\mathcal{R} = R_c^I$, we see that the applied averaging does not significantly change the quantity $\mathcal{P}_\mu$. Thus, the influence of the beam broadening is included in our expression (16) for the averaged probability as an appropriate mean effect.

In the present article we shall demonstrate that the expression (16), with the quantities $v_c(\mu, F)$ and $P_\mu(R_{\min}, v_{\perp 0}, F)$ obtained by the simultaneous treatment of the electron state and the projectile motion, reproduces the main features of the experimental signals without any fitting parameter.

1. *Discrete velocity distribution*

The simplest, but still instructive simulation of the experimental signal by expression (16) can be obtained for a discrete initial perpendicular velocity distribution

$$f(v_{\perp 0}) = \sum_{i=1}^{N} f_i \delta(v_{\perp 0} - v_{\perp 0 i}), \quad (18)$$

where $\delta(x)$ is the Dirac δ function and the "statistical" weights f_i satisfy the relation $\sum_{i=1}^{N} f_i = 1$. In this simple model, since $P_\mu(R_{\min}; v_{\perp 0}, F) = 1$, the averaged probability $\mathcal{P}_\mu(F)$ is given by

$$\mathcal{P}_\mu(F) = \sum_{i=1}^{N} f_i \Theta\mathbf{(}v_c(\mu, F) - v_{\perp 0 i}\mathbf{)}. \quad (19)$$

In the former equation we have $\Theta\mathbf{(}v_c(\mu, F) - v_{\perp 0 i}\mathbf{)} = \Theta\mathbf{(}F - F_c(\mu, v_{\perp 0 i})\mathbf{)}$.

To illustrate the results for discrete velocity distribution, one can take only the three representative velocities ($N = 3$) from the incident atomic beam: $v_{\perp 01} = 0.7 \times 10^{-5}$ a.u., $v_{\perp 02} = 1.4 \times 10^{-5}$ a.u., and $v_{\perp 03} = 2.1 \times 10^{-5}$ a.u. The velocity $v_{\perp 02} = \bar{v}$ represents the mean velocity of the beam, and the velocities $v_{\perp 01}$ and $v_{\perp 03}$ determine the width 2Δ of the initial perpendicular velocity distribution: $v_{\perp 03} - v_{\perp 01} = 2\Delta$. For

the corresponding weights f_i, we take the following values: $f_1 = 2/10$, $f_2 = 6/10$, and $f_3 = 2/10$. Therefore, using the notation $F_i = F_c(\mu, v_{\perp 0i})$, $i = 1, 2, 3$, from Eq. (19), we get $\mathcal{P}_\mu = 0$ for $F < F_1$, $\mathcal{P}_\mu = f_1 = 0.2$ for $F_1 \geqslant F < F_2$, $\mathcal{P}_\mu = f_1 + f_2 = 0.8$ for $F_2 \geqslant F < F_3$, and $\mathcal{P}_\mu = f_1 + f_2 + f_3 = 1$ for $F \geqslant F_3$.

In the special case $N = 1$ of the monoenergetic beam of the atomic particles in state μ with the initial perpendicular velocity $v_{\perp 0}$, we have

$$\mathcal{P}_\mu(F) = \Theta\big(F - F_c(\mu, v_{\perp 0})\big). \tag{20}$$

The signal rapidly appears for the field $F = F_c(\mu, v_{\perp 0})$; for this value of the external electric field, all atomic projectiles will be ionized and collected. The same situation holds for all $F > F_c(\mu, v_{\perp 0})$. In the idealized "experiment" with a monoenergetic beam, the minimal electric field $F_{\min}$ coincides with the critical field $F_c(\mu, v_{\perp 0})$. Thus, the simple steplike relation (14) gives the correct ionization distances.

In Fig. 8(a) we simulated the experimental signal using the discussed discrete initial perpendicular velocity distribution f with three representative velocities, considering the ionization of the atomic particles prepared in the Rydberg state $\mu = (n = 17, n_1 = 0, m = 0)$. The corresponding averaged probability $\mathcal{P}_\mu(F)$ given by Eq. (19) is shown as a dashed line. The values of the fields $F_i = F_c(\mu, v_{\perp 0i})$ in expression (19) are taken from Fig. 6. The probability $\mathcal{P}_\mu(F)$ is compared with the normalized experimental signal [symbols in Fig. 8(a)] [3].

From Fig. 8(a) we see that the minimal electric field $F_{\min} = 2.0 \times 10^{-7}$ a.u. obtained experimentally from the signal is less than the critical electric field $F_c(\mu, v_{\perp 01})$ at which the signal begins in the considered discrete velocity approximation. For that reason, as it was discussed in Sec. IV C, for the accurate calculation of R_c^I by Eq. (14) with the $F_{\min}$ value, it is necessary to use the lower initial perpendicular velocity ($v_{\perp 0} < v_{\perp 01}$), or to calculate the R_c^I values using, for example, the quantities $\bar{F}$ and $\bar{v}$. The qualitative agreement of the theoretical signal for discrete distribution f with the available experimental data, recognized in Fig. 8(a), can be used as a simple proof that relation (16) reflects the main physical features of the signal.

2. *Gaussian velocity distribution*

A more appropriate distribution f that can be used in the analysis of the signal under the real experimental conditions is the Gaussian distribution centered at $\bar{v}_{\perp 0} = \bar{v}$, with the half width Δ

$$f(v_{\perp 0}) = \frac{1}{\Delta\sqrt{\pi}} \exp\left[-\frac{(v_{\perp 0} - \bar{v})^2}{\Delta^2}\right]. \tag{21}$$

The typical values for the atomic beam used in experiment are $\bar{v} = v_{\perp 02} = 1.4 \times 10^{-5}$ a.u. and $\Delta = (v_{\perp 03} - v_{\perp 01})/2 = 0.7 \times 10^{-5}$ a.u. [3].

Inserting Eq. (21) into Eq. (16), and taking into account that $P_\mu(R_{\min}; v_{\perp 0}, F) \approx 1$, we obtain the averaged ionization probability in the simple form

$$\mathcal{P}_\mu(F) = \frac{1}{2}\left[1 + \mathrm{erf}\left(\frac{v_c(\mu, F) - \bar{v}}{\Delta}\right)\right], \tag{22}$$

where $\mathrm{erf}(x)$ is the error function. From Eq. (22) we recognize that the experimental signal appears as a consequence of a specific entanglement of the initial velocity distribution f (described by the quantities $\bar{v}$ and Δ) and quantum decay of the projectile. We recall that in the present article the ionization (decay) and the ionic motion have been considered simultaneously; the critical velocity $v_c(\mu, F)$ in Eq. (22) reflects the main properties (existence of $R_{\min}$) of the projectile motion in the external electric field F, governed by the probability $P_\mu(R)$. For a vary narrow distribution f, that is, for $\Delta \to 0$, from Eq. (22) we get $\mathcal{P}_\mu(F) = 0$ for $F < F_c(\mu, \bar{v})$ and $\mathcal{P}_\mu(F) = 1$ for $F \geqslant F_c(\mu, \bar{v})$; that is, we get the averaged probability expressed by Eq. (20).

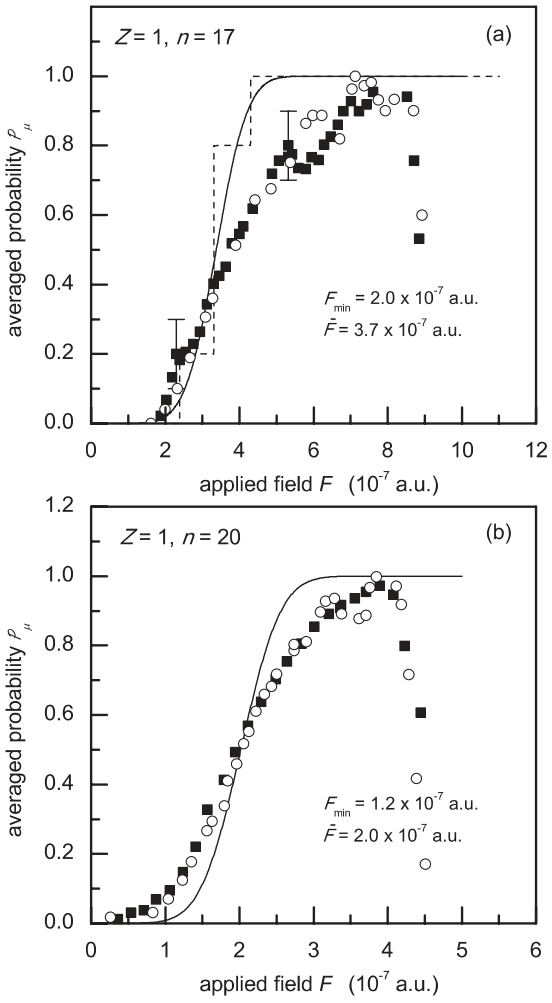

FIG. 8. Averaged ionization probabilities $\mathcal{P}_\mu(F)$ for (a) the H($n = 17$) and (b) the H($n = 20$) atomic projectiles for $n_1 = 0$ and $m = 0$ via the external electric field F. The dashed curve in (a) corresponds to the discrete initial perpendicular velocity distribution; the solid curves correspond to the Gaussian distribution f. Symbols (■ and ○) represent the experimental data for Xe($n = 17$) and Xe($n = 20$) [3].

In Fig. 8 we present the averaged ionization probabilities $\mathcal{P}_\mu(F)$ expressed by Eq. (22) (solid curves), using the values $v_c(\mu, F)$ from Fig. 6. In Figs. 8(a) and 8(b) we consider the cases $n = 17$ and $n = 20$ (for $n_1 = 0$ and $m = 0$), respectively, for which the normalized experimental signals are available (symbols in Fig. 8) [3]. In the experiments, the signal vanishes for $F > F_{\text{thr}}$; in Ref. [3] this effect has been connected with

the finite time window for detection of the ionized particles and a direct (field) ionization for $F > F_{\text{thr}}$. The theoretical curves begin at $F = F_{\text{min}}$, reaching the unit value $\mathcal{P} = 1$ for some characteristic larger fields. The mean field $\bar{F}$ can be defined by the relation $\mathcal{P}_\mu(\bar{F}) = 1/2$. The theoretical curves increase more rapidly with increasing F than the experimentally obtained curves (signal), but the values F_{min} and $\bar{F}$ [exposed explicitly in Figs. 8(a) and 8(b)] are in accord with experimental data.

The obtained qualitative agreement with experimental signals, and the agreement for the values F_{min} and $\bar{F}$ with the experimental ones, indicate that the EEM and the proposed formula (16) for the ion signal provide an explanation of all specific features of the ionization dynamics of the considered Rydberg states. The analysis of the present article also suggests that the experimental values F_{min} must be combined with the values $v_c(\mu, F_{\text{min}})$ if the expression (14) is used for the calculation of the ionization distances R_c^I, the main physical information about the intermediate stages of the process. As the values $v_c(\mu, F_{\text{min}})$ are not known experimentally, one can combine the experimentally available values $\bar{F}$ and $\bar{v}$ for more accurate derivation of the quantities R_c^I from the signal.

V. CONCLUDING REMARKS

In this article we consider the ionization dynamics of the beam of atomic particles impinging a conducting solid surface in the presence of a weak external electric field F. The recently developed EEM [13] has been applied to describe the intermediate stages of the electron transitions in the ion-surface system. In the present article, a kind of self-consistent procedure is proposed to include the ionic motion in the problem: The ionization probability $P_\mu(R)$ and the perpendicular velocity $v_\perp(R) = -dR/dt$ of the representative projectile of subensemble with a given initial velocity are calculated simultaneously.

The results are obtained for high-eccentricity Rydberg states of the active electron and in the region of low ionic velocities. The classification of the states by the parabolic quantum numbers $\mu = (n_1, n_2, m)$ follows the intermediate parabolic symmetry of the system. The accuracy of the EEM is tested by comparing with the available theoretical and experimental results. We compare our results with the WPP method [11,12] and the CSM one [9,14]. The normalized experimental signal [3] is compared with the averaged ionization probability $\mathcal{P}_\mu(F)$. An agreement with both the theoretical and the experimental results means that the EEM, which belongs to the class of asymptotic methods, provides very useful information, providing that it is *ab initio* formulated in the critical region $R \approx R_c \approx R_c^I$ of the ion-surface distances.

According to the analysis of the present article, the experimental signal appears as the consequence of a specific entanglement of the initial velocity distribution f within the projectile beam and the character of the (representative) projectile motion in the external electric field F, governed by the probability $P_\mu(R)$, which is expressed by the parameter $v_c(\mu, F)$. The theoretical analysis of the present article gives the ionization distances R_c^I for all $v_{\perp 0}$ and F. These values are in accord with the values deduced from the steplike formula (14), providing that the values of the external electric field F are combined with the values $v_{\perp 0} = v_c(\mu, F)$ of the incident perpendicular velocity.

The same formula could be used for deducing the ionization distances R_c^I from the fields $F = F_{\text{min}}$ (known from the experimental signal) if the corresponding values $v_c(\mu, F_{\text{min}})$ are known. Because those values are not known, we suggested that the sufficiently accurate R_c^I values can be obtained from Eq. (14) for the combination of the mean fields $\bar{F}$ and the mean values $\bar{v}$ of the initial perpendicular velocities, both known experimentally. In the further elaboration of this problem, the normalized experimental signals for Rydberg states other than those considered in Ref. [3] would be of interest. We point out that if the normalized experimental signal is simulated by Eq. (22), one can fit the critical velocity by the function $v_c = \alpha\sqrt{F} - \beta$; from the coefficients α and β thus deduced from the experiment, the ionization distances (for $Z = 1$) can be calculated from the relation $R_c^I = \alpha/2\beta$ [see Eq. (15)].

A few additional concluding comments may be relevant for further investigations of the signal and the related R_c^I problem, from both the theoretical and the experimental points of view.

First, the used EEM is developed for the pointlike projectiles and the conducting solid surfaces. On the other hand, the experiments were performed with Xe Rydberg atoms and for the variety of different solid surfaces: the conducting surfaces [1–3], the dielectric surfaces [4], the surfaces with localized stray fields [6], and the robust surfaces [7]. In the case of conducting surfaces, the considerations of the present article can be adapted to the real experimental conditions by taking into account the polarization of the ionic core of an Xe atom. This polarization is due to the internal electronic structure of the atom (quantum defects associated with the low-l states) and also to the applied external electric field F and the influence of the polarized solid. All these effects can be taken into account via effective core charge $Z_{\text{eff}} \neq 1$, or more exactly via the appropriate effective potentials. Recently, it was demonstrated that the core polarization induces a shift of the rates toward the smaller ion-surface distances [17], which means that the EEM predictions with polarization of the ionic cores taken into account will be in a better agreement with the WPP findings. The influence of the type of the solid surface to the ionization process can be also included in the model via the analytical continuation of the function Ψ_μ from the barrier into the solid region.

Second, the proposed theoretical explanation of the experimental signal can be applied to different ion-surface geometries and/or different projectile beams. Our preliminary calculations show that the change of the angle of incidence (due to the shift of the distribution f), results in the shift of the averaged probability $\mathcal{P}_\mu$. On the other hand, the increase of the width Δ of the distribution f results in the less rapid increase of the function $\mathcal{P}_\mu$ with increasing F, etc. By modeling the position and the shape of the distribution f, one can obtain the better agreement of the averaged probability with the experimental signal and vice versa.

Third, the ionization distances R_c^I of the atomic projectile for parabolic quantum numbers $n_1 \simeq n - 1$ and $m = 0$ were not discussed in the present article. These Rydberg states

can also be consistently treated within the EEM exposed in the present article, because they are of the "low-l" type. However, the electron transitions between adiabatic decaying states must be taken into account in that case. We point out that some experimental data [2] indicate that the R_c^I values of high-lying Xe(n) Stark manifolds are similar for $n_1 = 0$ and $n_1 = n - 1$ for $m = 0$. A first theoretical analysis of this fact, based on the model of avoided crossings, already exists [2,18], but the analysis using the EEM energy terms and rates can provide a more consistent explanation (because the terms obtained in the present article are molecularlike).

Finally, for lower values of the applied filed, the experimental signal can be simulated more accurately by taking into account the fact that in some cases the ionization is incomplete; that is, $P_\mu(R_{\min}; v_{\perp 0}, F) < 1$. The theoretical explanation of the behavior of the signal in the near-threshold region of the applied electric field ($F \lesssim F_{\text{thr}}$) requires additional analysis.

ACKNOWLEDGMENTS

This work was supported in part by the Ministry of Science and Technological Development, Republic of Serbia (Project 14 1029).

[1] S. B. Hill, C. B. Haich, Z. Zhou, P. Nordlander, and F. B. Dunning, Phys. Rev. Lett. **85**, 5444 (2000).
[2] Z. Zhou, C. Oubre, S. B. Hill, P. Nordlander, and F. B. Dunning, Nucl. Instrum. Methods Phys. Res. B **193**, 403 (2002).
[3] S. Wethekam, H. R. Dunham, J. C. Lancaster, and F. B. Dunning, Phys. Rev. A **73**, 032903 (2006).
[4] H. R. Dunham, S. Wethekam, J. C. Lancaster, and F. B. Dunning, Nucl. Instrum. Methods Phys. Res. B **256**, 46 (2007).
[5] F. B. Dunning, S. Wethekam, H. R. Dunham, and J. C. Lancaster, Nucl. Instrum. Methods Phys. Res. B **258**, 61 (2007).
[6] D. D. Neufeld, H. R. Dunham, S. Wethekam, J. C. Lancaster, and F. B. Dunning, Phys. Rev. B **78**, 115423 (2008).
[7] D. D. Neufeld, H. R. Dunham, S. Wethekam, J. C. Lancaster, and F. B. Dunning, Surf. Sci. **602**, 1306 (2008).
[8] G. R. Lloyd, S. R. Procter, and T. P. Softley, Phys. Rev. Lett. **95**, 133202 (2005).
[9] P. Nordlander and F. B. Dunning, Phys. Rev. B **53**, 8083 (1996).
[10] J. Hanssen, C. F. Martin, and P. Nordlander, Surf. Sci. **423**, L271 (1999).
[11] J. Sjakste, A. G. Borisov, and J. P. Gauyacq, Phys. Rev. A **73**, 042903 (2006).
[12] E. So, M. T. Bell, and T. P. Softley, Phys. Rev. A **79**, 012901 (2009).
[13] N. N. Nedeljković and Lj. D. Nedeljković, Phys. Rev. A **72**, 032901 (2005).
[14] J. Braun and P. Nordlander, Surf. Sci. **448**, L193 (2000).
[15] Lj. D. Nedeljković, N. N. Nedeljković, and D. K. Božanić, Phys. Rev. A **74**, 032901 (2006).
[16] P. Nordlander, Phys. Rev. B **53**, 4125 (1996).
[17] N. N. Nedeljković and M. D. Majkić, Phys. Rev. A **76**, 042902 (2007).
[18] F. B. Dunning, H. R. Dunham, C. Oubre, and P. Nordlander, Nucl. Instrum. Methods Phys. Res. B **203**, 69 (2003).